Effects of Soret, Dufour, chemical reaction, thermal radiation and volumentric heat generation/absorption on mixed convection stagnation point flow on an Iso-thermal vertical plate in porous media

Olanrewaju, P.O. and Gbadeyan, J.A.
Department of Mathematics,
Covenant University, Ota, Ogun State. Nigeria.

*E-mail: aoladapo_anu@yahoo.ie, Philip.olanrewaju@covenantuniversity.edu.ng

ABSTRACT

A mathematical model is analyzed in order to study the effects of Soret, Dufour, chemical reaction, thermal radiation and volumentric heat generation/absorption on mixed convection stagnation point flow on an Iso-thermal vertical plate in a porous media. The governing partial differential equations are transformed into set of coupled ordinary differential equations, which are solved numerically using Runge-Kutta sixth order method along with shooting technique. The physical interpretation to this expression is assigned through graphs and tables for the wall shear stress $f''(0)$, Nusselt number $-\theta'(0)$ and Sherwood number $-\phi'(0)$. Results were compared with the existing literature and showed a perfect agreement. Similarly, results showed that the fields were influenced appreciably by the effects of the governing parameters: Soret number Sr, Dufour number D_f, chemical reaction parameter γ, thermal radiation parameter Ra, order of reactions n, thermal Grashof number G_T, solutal Grashof number G_C, Prandtl number Pr, permeability parameter K, rate of heat generation/absorption parameter S, and magnetic field strength parameter M. It was evident that for some kind of mixtures such as the light and medium molecular weight, the Soret and Dufour's effects should be considered as well.

(Keywords: Soret number; Dufour number; Chemical reaction; Thermal radiation; Volumentric rate of heat generation/absorption; Stagnation point flow; Heat and mass transfer.

9)

INTRODUCTION

Convective heat transfer in porous media has been a subject of great interest for the last several decades. The research activities in this field has been accelerated because of a broad range of applications in various disciplines, such as geophysical, thermal and insulating engineering, modelling of packed sphere beds, solar power collector, pollutant dispersion in aquifers, cooling of electronic systems, ventilation of rooms, crystal growth in liquids, chemical catalytic reactors, grain storage devices, petroleum reservoirs, ground hydrology, fiber and granular insulation, nuclear waste repositories, high-performance building insulation, post-accident heat removal from pebble-bed nuclear reactors, concepts of aerodynamics heat shielding with transpiration cooling, etc. (see [1], [2-3], [4-5]) . In fluid dynamics, a stagnation point is a point in a flow field where the local velocity of the fluid is zero. Stagnation points exist at the surface of objects in the flow field, where the fluid is brought to rest by the object. A stagnation point occurs whenever a flow impinges on a solid object. Usually there are other important features of the flow.

Singh et al. [6], investigated the effect of volumentric heat generation/absorption on mixed convection stagnation point flow on an Iso-thermal vertical plate in porous media. The volumentric rate of heat generation Q [Watt/m^3] in the boundary layer flows generally has been presented in the literature (see, [7, 8, 9]). Shateyi et al. [10], examined the effects of thermal radiation, hall currents, Soret, and Dufour on MHD flow by mixed convection over a vertical surface in porous media. It is worth also mentioning that radiation effects on the convective flow are important in the context of space technology and process involving high temperatures.

Pop [11] have investigated the effects of radiation on mixed convection flow over a vertical pin, whereas Mohammedein and El-Amin [12] studied the problem of thermal dispersion and radiation effects on non-Darcy natural convection in a fluid-saturated porous medium. Thermal radiation heat transfer effects on the Rayleigh of gray viscous fluids under the effect of a transverse magnetic field have been investigated by Duwairi and Duwairi [13]. Pop et al. [14] investigated the steady two-dimensional stagnation-point flow of an incompressible fluid over a stretching sheet by taking into account radiation effects using the Rosselland approximation to model the heat transfer. Hayat et al [15] studied heat and mass transfer for Soret and Dufour's effect on mixed convection boundary layer flow over a stretching vertical surface in a porous medium filled with a viscoelastic fluid. [16], investigated mixed convection in the stagnation-point flow of a Maxwell fluid towards a vertical stretching surface.

The aim of the present paper is, therefore, the influence of Soret, Dufour, chemical reaction, thermal radiation and volumentric heat generation/absorption on mixed convection stagnation point flow on an Iso-thermal vertical plate in porous media which is an extension of Singh et al [6]. With the knowledge of the authors, this research work has not been carried out by any researcher. We also consider the local species concentration as a factor of the volumentric rate of heat generation. To study this model, a stagnation point flow was chosen, which had been studied earlier to understand flow pattern which varies from clear fluid flow to highly porous flow. The rest of the paper is structured as follows. In section 2, we formulate the problem; in section3, we give the method of solution. Our results are presented and discussed in section 4, and in section 5, we present some brief conclusions.

MATERIALS AND METHODS

Basic Theory

Consider steady laminar stagnation point flow of a viscous incompressible fluid through porous media along a vertical isothermal plate in the presence of volumentric rate of heat generation and magnetic field. The x-axis is taken along the plate and y-axis is normal to the plate and the flow is confined in half plane y > 0. The potential flow arrives from the y-axis and impinges on plate, which divides at stagnation point into two streams and the viscous flow adheres to the plate. The velocity distribution in the potential flow is given by $U_\infty = cx$ and $V_\infty = cy$, where c is a positive constant. Following Singh et al. [6] the linear Darcy term representing distributed body force due to porous media is retained while the non-linear Forchheimer term is neglected, thus the governing equations of continuity, momentum, energy and specie are given by

$$\frac{\partial u}{\partial x}+\frac{\partial v}{\partial y}=0 \quad (1)$$

$$u\frac{\partial u}{\partial x}+v\frac{\partial u}{\partial y}=\upsilon\frac{\partial^2 u}{\partial y^2}+g\beta(T-T_\infty)+g\beta^*(C-C_\infty)-\frac{\sigma_e B_0^2}{\rho}(u-U \quad (2)$$

$$u\frac{\partial T}{\partial x}+v\frac{\partial T}{\partial y}=\alpha\frac{\partial^2 T}{\partial y^2}-\frac{\alpha}{k}\frac{\partial q_r}{\partial y}+Q(T-T_\infty)+\frac{D_e k_T}{c_s c_p}\frac{\partial^2 C}{\partial y^2} \quad (3)$$

$$u\frac{\partial C}{\partial x}+v\frac{\partial C}{\partial y}=D_e\frac{\partial^2 C}{\partial y^2}+\frac{D_e k_T}{T_m}\frac{\partial^2 T}{\partial y^2}-k_1(C-C_\infty)^n \quad (4)$$

,

subject to the boundary conditions

$$v=0,\ u=0,\ T=T_w,\ C=C_w \quad \text{at} \quad y=0 \quad (5)$$

$$u\to U_\infty=cx,\ T\to T_\infty,\ C\to C_\infty \quad \text{as } y\to\infty \quad (6)$$

Where u and v are the velocity components in the x- and y-directions, respectively, ρ is the fluid density, υ is the kinematic viscosity, σ_e is the electrical conductivity of the fluid, $\widetilde{K}$ is the permeability of the porous medium, g is the gravitational acceleration, β is the thermal expansion coefficient, β^* is the coefficient of expansion with concentration, T is the temperature, c_p is the specific heat capacity at constant pressure of the fluid, α is the thermal conductivity of the fluid, q_r is the radiative heat flux, T_w is the temperature of the plate, Q is the volumentric rate heat

generation/absorption, B_0 is the magnetic field of constant strength, D_e is the coefficient of mass diffusivity, c_s is the concentration susceptibility, k_1 is the rate of chemical reaction, n is the order of reaction respectively.

The radiative heat flux q_r is described by Roseland approximation such that

$$q_r = -\frac{4\sigma^*}{3K'}\frac{\partial T^4}{\partial y}, \tag{7}$$

where σ^* and K' are the Stefan-Boltzmann constant and the mean absorption coefficient, respectively. Following Shateyi et al. [10], we assume that the temperature differences within the flow are sufficiently small so that the T^4 can be expressed as a linear function after using Taylor series to expand T^4 about the free stream temperature T_∞ and neglecting higher-order terms. This result is the following approximation:

$$T^4 \approx 4T_\infty^3 T - 3T_\infty^4. \tag{8}$$

Using (7) and (8) in (3), we obtain

$$\frac{\partial q_r}{\partial y} = -\frac{16\sigma^*}{3K}\frac{\partial T^4}{\partial y}. \tag{9}$$

Following Alam and Rahman. [17], we nondimensionalize (1)-(4) using the following transformations:

$$\theta(\eta) = \frac{T - T_\infty}{T_w - T_\infty}, \quad \phi(\eta) = \frac{C - C_\infty}{C_w - C_w}, \tag{10}$$

where $f(\eta)$ is the dimensionless stream function and ψ is the dimensionless stream function defined by $u = \frac{\partial \psi}{\partial x}$ and $v = -\frac{\partial \psi}{\partial y}$, just to satisfy the equation of continuity (1).

Where $\psi(x, y) = \sqrt{c\upsilon}\, x f(\eta)$ and $\eta = y\sqrt{\frac{c}{\upsilon}}$. (11)

Substituting eq. (9) into the eq. (3), then eq. (11) into the eqs. (2), (3) and (4), the resulting non-linear ordinary differential equations are

$$f''' + ff'' - f'^2 + G_T\theta + G_c\phi - (K + M)(f' - 1) + 1 = 0, \tag{12}$$

$$\left(1 + \frac{4}{3}Ra\right)\theta'' + \Pr f\theta' + S\phi + \Pr D_f\phi'' = 0, \tag{13}$$

$$\phi'' + Scf\theta' + ScSr\theta'' - Sc\gamma\phi^n = 0, \tag{14}$$

with the boundary conditions

$$f = 0, \quad f' = 0, \quad \theta = 1, \quad \phi = 1 \quad at \quad \eta = 0,$$
$$f' = 1, \quad \theta = 0, \quad \phi = 0 \quad as \quad \eta \to \infty. \tag{15}$$

Where the primes denote differentiation with respect to η.

Where $M = \frac{\sigma B_0^2}{\rho c}$ is the magnetic parameter,

$\Pr = \frac{\upsilon}{\alpha}$ is the Prandtl number, $Sc = \frac{\upsilon}{D_e}$ is the Schmidt number, $Sr = \frac{D_e k_T (T_w - T_\infty)}{\upsilon T_m (C_w - C_\infty)}$ is the Soret number,

$D_f = \frac{D_e k_T (C_w - C_\infty)}{\upsilon c_s c_p (T_w - T_\infty)}$ is the Dufour number,

$G_T = \frac{g\beta(T_w - T_\infty)}{U_\infty c}$ is the local thermal Grashof number, $G_C = \frac{g\beta^*(C_w - C_\infty)}{U_\infty c}$ is the local solutal Grashof number, K is the permeability parameter, γ is the chemical reaction parameter, Ra is the radiation parameter and S is the rate of heat generation/absorption parameter respectively.

Computational procedure

The set of Eqs. (12)-(14) together with the boundary conditions (15) have been solved numerically by applying Nachtsheim-Swigert shooting iteration technique along with Runge-Kutta sixth-order integration method. From the

process of numerical computation, the skin-friction coefficient, the local Nusselt number and the local Sherwood number, which are respectively proportional to $f''(0), -\theta'(0)$ *and* $-\phi'(0)$, are also sorted out and their numerical values are presented in a tabular form. The computations have been performed by a program which uses a symbolic and computational computer language MAPLE [18]. A step size of $\Delta\eta = 0.001$ is selected to be satisfactory for a convergence criterion of 10^{-7} in nearly all cases. The value of y_∞ is found to each iteration loop by the assignment statement $\eta_\infty = \eta_\infty + \Delta\eta$. The maximum value of η_∞, to each group of parameters, *Pr*, *Sc*, *Sr*, D_f, *M*, *Ra*, G_T, G_C, K, S and γ is determined when the values of unknown boundary conditions at η = 0 do not change to successful loop with error less than 10^{-7}.

RESULTS AND DISCUSSION

In order to get a clear insight of the physical problem, the velocity, temperature and concentration have been discussed by assigning numerical values to the parameters encountered in the problem. To be realistic, the values of the embedded parameters were chosen following Singh et al. [6]. Attention is focused on positive values of the buoyancy parameters i.e. Grashof number $G_T > 0$ (which corresponds to the cooling problem) and solutal Grashof number $G_C > 0$ (which indicates that the chemical species concentration in the free stream region is less than the concentration at the boundary surface). The cooling problem is often encountered in engineering applications. In table 1, comparison is made for some fixed parameters and there is a perfect agreement with Singh et al. [6] which is a special case of ours. We went further in table 2 to generate the skin friction coefficient, Nusselt number and the Sherwood number for some embedded parameters value in the flow model. Here, the values of Dufour number and Soret number are chosen so that their product is constant provided that the mean temperature is also kept constant. It is clearly seen that an increase in the parameters M, S, Ra, G_T, G_C, K, D_f, Sr, and n leads to an increase in the skin-friction at the wall plate while increase in parameters Pr, S and Sc decreases the skin-friction at the wall surface. Similarly, the Nusselt number coefficient increases at the wall plate when G_T, G_C, Pr, Ra, K, M, and γ increases while it decreases at the wall plate when parameters S, Df, Sr, Sc and n increases. It is interesting to note that Sherwood number at the wall plate increases with increase in S, M, D_f, Sr and γ and decreases with other parameters embedded in the flow model.

Table 1

Computations showing values of $f''(0)$, $-\theta'(0)$, $-\phi'(0)$ for different values of S when $G_T = 1.0$, $G_C = 0.5$, Pr = 1, Sc = 0.5, M = 0, Ra = 0, K = 0, $D_f = 0$, Sr = 0, $\gamma = 0$, n = 0.

	Singh et al [6]	Singh et al [6]	Singh et al [6]	Present	Present	Present
S	$f''(0)$	$-\theta'(0)$	$-\phi'(0)$	$f''(0)$	$-\theta'(0)$	$-\phi'(0)$
-1	1.8444	1.3908	0.4631	1.844462	1.390856	0.463174
0	1.9995	0.6392	0.4789	1.999553	0.639244	0.478964
1	2.1342	-0.0730	0.4919	2.134287	-0.073040	0.491749

Table 2

Computations showing values of $f''(0)$, $-\theta'(0)$, $-\phi'(0)$ for various parameters embedded in the flow model.

S	K	Pr	G_T	G_C	Sc	M	Ra	D_f	Sr	γ	n	$f''(0)$	$-\theta'(0)$	$-\phi'(0)$
-1	1	1	1	0.5	0.5	0.1	0.1	0.03	2	1	1	2.170013	1.297714	0.432545
0	1	1	1	0.5	0.5	0.1	0.1	0.03	2	1	1	2.251354	0.600052	0.935779
1	1	1	1	0.5	0.5	0.1	0.1	0.03	2	1	1	2.310142	0.072134	1.321194
1	3	1	1	0.5	0.5	0.1	0.1	0.03	2	1	1	2.707940	0.080941	1.319387
1	5	1	1	0.5	0.5	0.1	0.1	0.03	2	1	1	3.055692	3.055692	1.317981
1	1	3	1	0.5	0.5	0.1	0.1	0.03	2	1	1	2.244907	0.423668	1.127455
1	1	10	1	0.5	0.5	0.1	0.1	0.03	2	1	1	2.192064	0.845524	0.833095
1	1	1	1.5	0.5	0.5	0.1	0.1	0.03	2	1	1	2.548931	0.092862	1.316342
1	1	1	2	0.5	0.5	0.1	0.1	0.03	2	1	1	2.780013	0.111901	1.311819
1	1	1	1	1	0.5	0.1	0.1	0.03	2	1	1	2.488093	0.086051	1.317992
1	1	1	1	2	0.5	0.1	0.1	0.03	2	1	1	2.842183	0.113033	1.311677
1	1	1	1	0.5	1	0.1	0.1	0.03	2	1	1	2.301017	0.081146	1.610442
1	1	1	1	0.5	2	0.1	0.1	0.03	2	1	1	2.286417	0.094415	2.135008
1	1	1	1	0.5	0.5	1	0.1	0.03	2	1	1	2.496652	0.076377	1.320322
1	1	1	1	0.5	0.5	3	0.1	0.03	2	1	1	2.869562	0.084245	1.318713
1	1	1	1	0.5	0.5	0.1	1	0.03	2	1	1	2.323174	0.168204	1.194747
1	1	1	1	0.5	0.5	0.1	3	0.03	2	1	1	2.342316	0.185900	1.132473
1	1	1	1	0.5	0.5	0.1	0.1	0.15	2	1	1	2.327828	0.124813	1.226749
1	1	1	1	0.5	0.5	0.1	0.1	0.60	2	1	1	2.346970	-0.07117	1.375710
1	1	1	1	0.5	0.5	0.1	0.1	0.03	4	1	1	2.329921	0.146990	1.324422
1	1	1	1	0.5	0.5	0.1	0.1	0.03	6	1	1	2.334231	0.129986	1.458411
1	1	1	1	0.5	0.5	0.1	0.1	0.03	2	3	1	2.270000	0.238037	1.864005
1	1	1	1	0.5	0.5	0.1	0.1	0.03	2	5	1	2.244893	0.265971	2.347379
1	1	1	1	0.5	0.5	0.1	0.1	0.03	2	1	2	2.356481	0.113188	1.039430
1	1	1	1	0.5	0.5	0.1	0.1	0.03	2	1	5	2.383374	0.072507	0.861491
1	1	1	1	0.5	0.5	0.1	0.1	0.03	2	1	6	2.386265	0.068600	0.833309

A. Velocity profiles

The effects of various thermophysical parameters on the fluid velocity are illustrated in Figs. 1 to 8. Fig. 1 depicts the effect of parameter S on the fluid velocity and we observed an increase in the fluid velocity as parameter S increases. This is because an increase in the volumentric rate of generation connotes increase in buoyancy force thereby increasing fluid velocity. It is interesting to note that Prandtl number and radiation parameter has little or no influence on the fluid velocity (see figs. 2 and 4). It is also interesting to note that increase in magnetic strength M and permeability parameters K increases the fluid velocity for $S = 0$ (see figs. 3 and 7). Figs. 5 and 6 depict the effect of the thermal and solutal Grashof numbers (G_T and G_C) on the fluid velocity within the boundary layer. The fluid velocity is highest at $\eta = 1.5$ for the highest values of G_T and G_C. However, the momentum boundary layer thickness generally increases as the parameter values of G_T and G_C increases for $S = 0$.

B. Temperature profiles

The influences of various embedded parameters on the fluid temperature are illustrated in Figs. 9 to 14. Increase in parameter S increases the thermal boundary layer thickness across the plate. It is interesting to note that for $S = 1$ and 2, there are sudden increase close to the wall plate before decreasing to satisfy the boundary condition at the free stream (see fig. 9). In fig. 10, it is seen that increase in Prandtl number Pr decreases the temperature profile and thereby decreases the thermal boundary layer thickness. At high Prandtl fluid has low velocity, which in turn also implies that at lower fluid velocity the specie diffusion is comparatively lower and hence higher specie concentration is observed at high Prandtl number. In figs. 11 and 14, increase in radiation parameter and Dufour number increases the thermal boundary layer thickness while in figs. 12 and 13, increase in thermal and solutal Grashof numbers decreases the thermal boundary layer thickness across the plate.

C. Concentration profiles

The effects of various thermophysical parameters on the fluid concentration are illustrated in Figs. 15 to 21. Fig. 15 reflects that with increase in Schmidt number Sc the fluid concentration decreases. Figs. 16 and 17 depict the effect of various values of the thermal and solutal Grashof numbers on the concentration boundary layer thickness. It is interesting to note that increase in this parameters bring a small decrease across the plate. In fig. 18, we display the graph of concentration profile against spanwise coordinate η for various values of Soret numbers Sr. It is noteworthy that increase in this parameter increases the concentration boundary layer thickness. It is interesting to note that there was a sudden increase close to the wall plate when $Sr = 10$ before satisfying the boundary condition at the free stream. It clearly seen that for a destructive chemical reaction parameter the concentration boundary layer thickness decreases while for productive chemical reaction parameter increases the concentration boundary layer thickness (see figs. 19 and 20). The order of the reaction n has little effects on the concentration boundary layer thickness. Increases in n leads to a small decrease in the concentration profile across the boundary layer (see fig. 21).

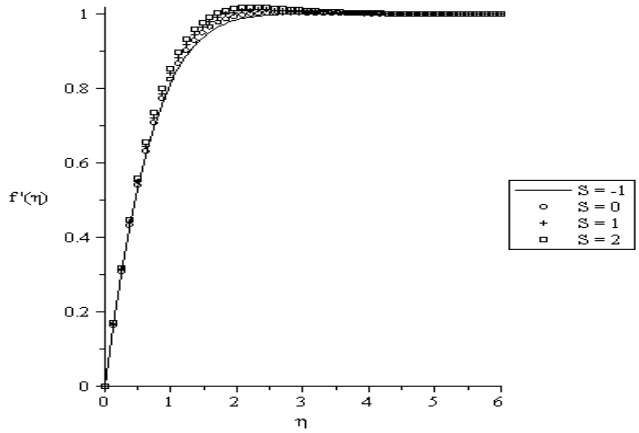

Figure 1: Velocity profiles for $G_T = 0.1$, $G_C = 0.1$, $K = 0.1$, $Pr = 0.71$, $Sc = 0.22$, $M = 0.1$, $Ra = 0.1$, $Sr = 2$, $D_f = 0.03$, $\gamma = 1$, $n = 1$.

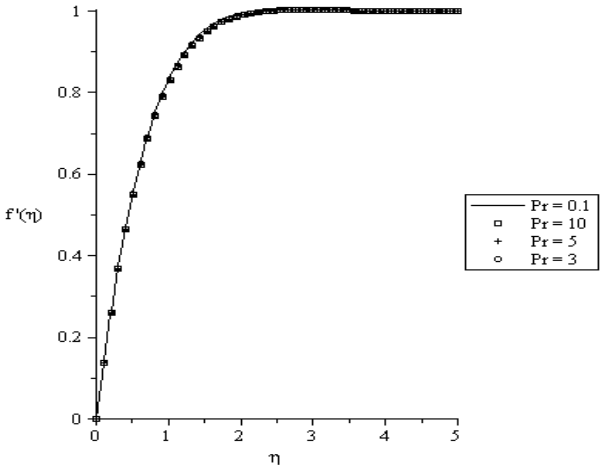

Figure 2: Velocity profiles for $G_T = 0.1$, $G_C = 0.1$, K = 0.1, S = 0, Sc = 0.22, M = 0.1, Ra = 0.1, Sr = 2, $D_f = 0.03$, $\gamma = 1$, n = 1.

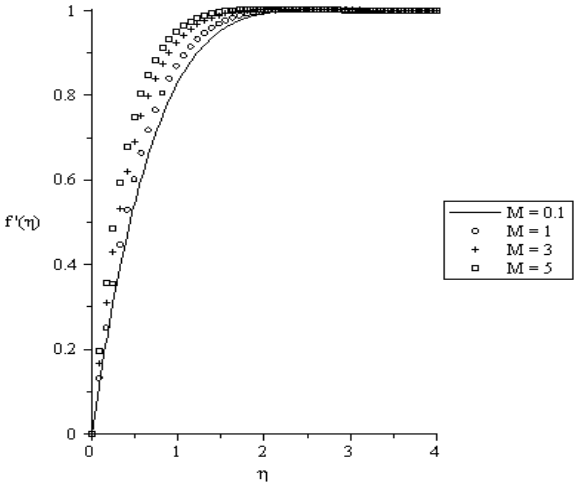

Figure 3: Velocity profiles for $G_T = 0.1$, $G_C = 0.1$, K = 0.1, S = 0, Pr = 0.71, Sc = 0.22, Ra = 0.1, Sr = 2, $D_f = 0.03$, $\gamma = 1$, n = 1.

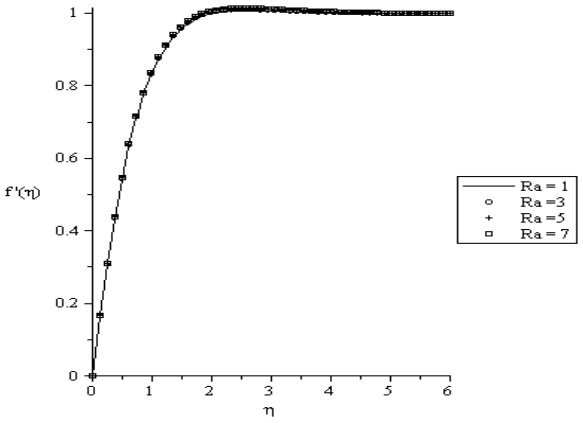

Figure 4: Velocity profiles for $G_T = 0.1$, $G_C = 0.1$, K = 0.1, S = 0, Pr = 0.71, Sc = 0.22, M = 0.1, Sr = 2, $D_f = 0.03$, $\gamma = 1$, n = 1.

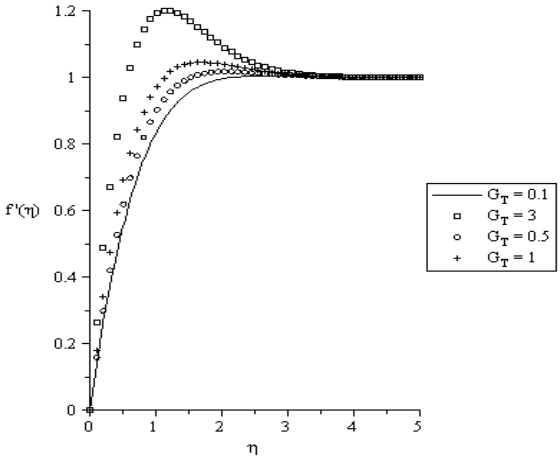

Figure 5: Velocity profiles for Ra = 0.1, $G_C = 0.1$, K = 0.1, S = 0, Pr = 0.71, Sc = 0.22, M = 0.1, Sr = 2, $D_f = 0.03$, $\gamma = 1$, n = 1.

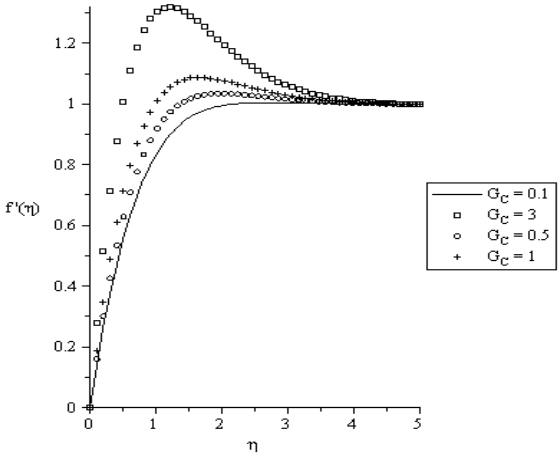

Figure 6: Velocity profiles for Ra = 0.1, $G_T = 0.1$, K = 0.1, S = 0, Pr = 0.71, Sc = 0.22, M = 0.1, Sr = 2, $D_f = 0.03$, $\gamma = 1$, n = 1.

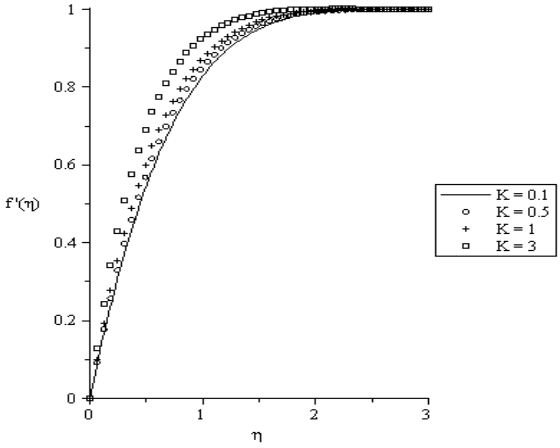

Figure 7: Velocity profiles for Ra = 0.1, $G_T = 0.1$, $G_C = 0.1$, S = 0, Pr = 0.71, Sc = 0.22, M = 0.1, Sr = 2, $D_f = 0.03$, $\gamma = 1$, n = 1.

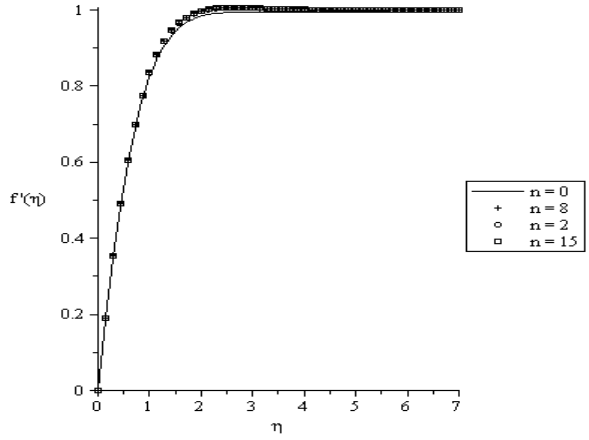

Figure 8: Velocity profiles for Ra = 0.1, G_T = 0.1, G_C = 0.1, S = 0, Pr = 0.71, Sc = 0.22, M = 0.1, D_f = 2, K = 0.1, Sr = 0.1, γ = 1.

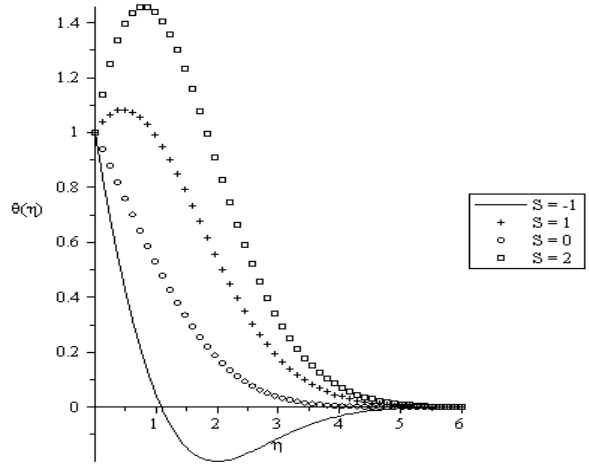

Figure 9: Temperature profiles for G_T = 0.1, G_C = 0.1, K = 0.1, Pr = 0.71, Sc = 0.22, M = 0.1, Ra = 0.1, Sr = 2, D_f = 0.03, γ = 1, n = 1.

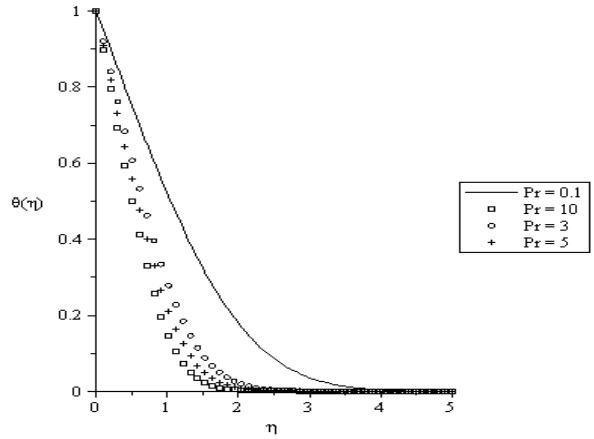

Figure 10: Temperature profiles for G_T = 0.1, G_C = 0.1, K = 0.1, S = 0, Sc = 0.22, M = 0.1, Ra = 0.1, Sr = 2, D_f = 0.03, γ = 1, n = 1.

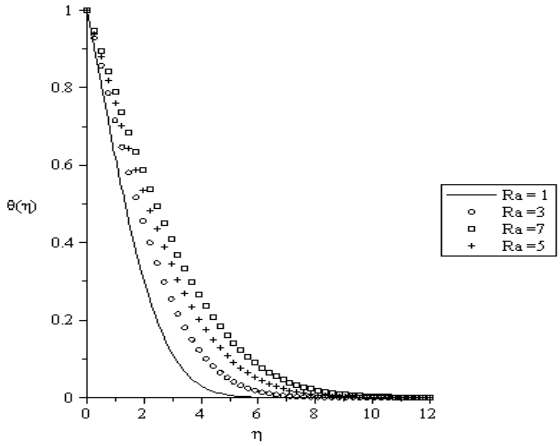

Figure 11: Temperature profiles for G_T = 0.1, G_C = 0.1, K = 0.1, S = 0, Pr = 0.71, Sc = 0.22, M = 0.1, Sr = 2, D_f = 0.03, γ = 1, n = 1.

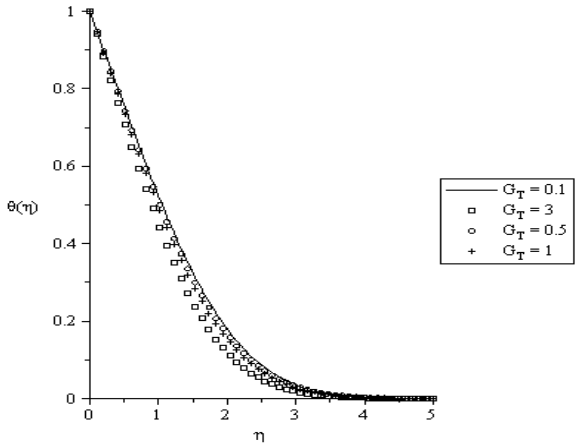

Figure 12: Temperature profiles for Ra = 0.1, G_C = 0.1, K = 0.1, S = 0, Pr = 0.71, Sc = 0.22, M = 0.1, Sr = 2, D_f = 0.03, γ = 1, n = 1.

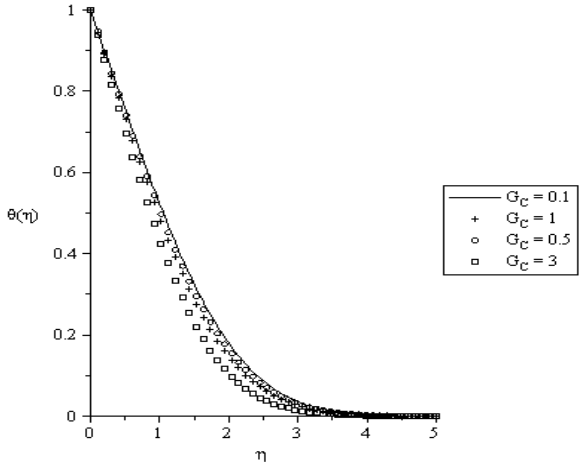

Figure 13: Temperature profiles for Ra = 0.1, G_T = 0.1, K = 0.1, S = 0, Pr = 0.71, Sc = 0.22, M = 0.1, Sr = 2, D_f = 0.03, γ = 1, n = 1.

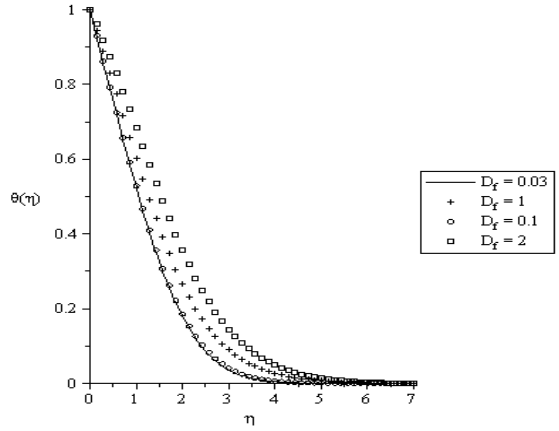

Figure 14: Velocity profiles for Ra = 0.1, G_T = 0.1, G_C = 0.1, S = 0, Pr = 0.71, Sc = 0.22, M = 0.1, Sr = 2, K = 0.1, γ = 1, n = 1.

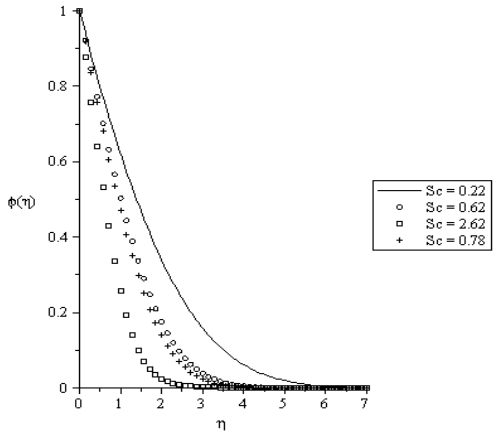

Figure15: Concentration profiles for G_T = 0.1, G_C = 0.1, K = 0.1, S = 0, Pr = 0.71, M = 0.1, Ra = 0.1, Sr = 2, D_f = 0.03, γ = 1, n = 1.

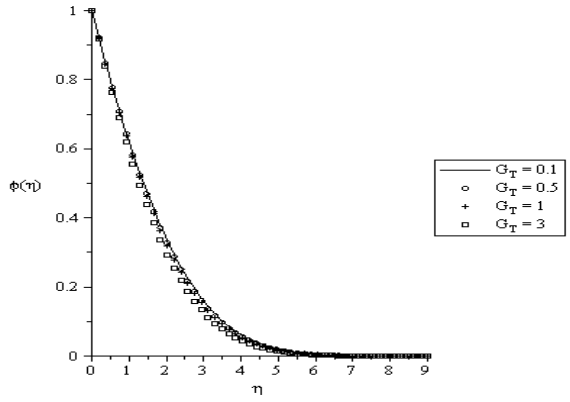

Figure 16: Concentration profiles for Ra = 0.1, G_C = 0.1, K = 0.1, S = 0, Pr = 0.71, Sc = 0.22, M = 0.1, Sr = 2, D_f = 0.03, γ = 1, n = 1.

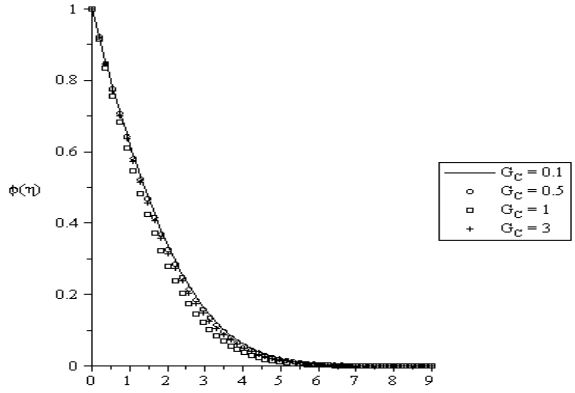

Figure 17 : Concentration profiles for Ra = 0.1, G_T = 0.1, K = 0.1, S = 0, Pr = 0.71, Sc = 0.22, M = 0.1, Sr = 2, D_f = 0.03, γ = 1, n = 1.

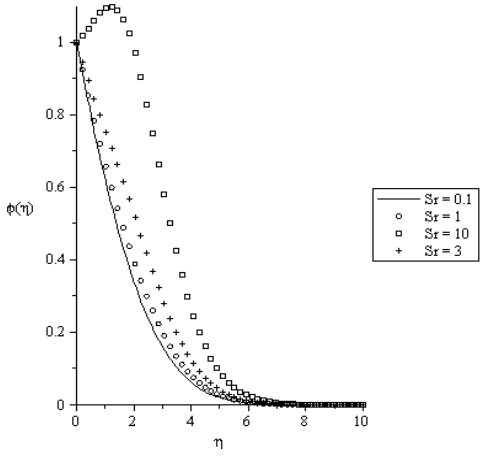

Figure 18: Concentration profiles for Ra = 0.1, G_T = 0.1, G_C = 0.1, S = 0, Pr = 0.71, Sc = 0.22, M = 0.1, D_f = 2, K = 0.1, γ = 1, n = 1.

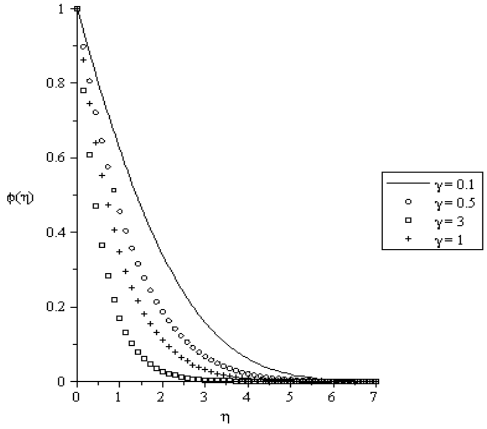

Figure 19: Concentration profiles for Ra = 0.1, G_T = 0.1, G_C = 0.1, S = 0, Pr = 0.71, Sc = 0.22, M = 0.1, D_f = 2, K = 0.1, Sr = 0.1, n = 1.

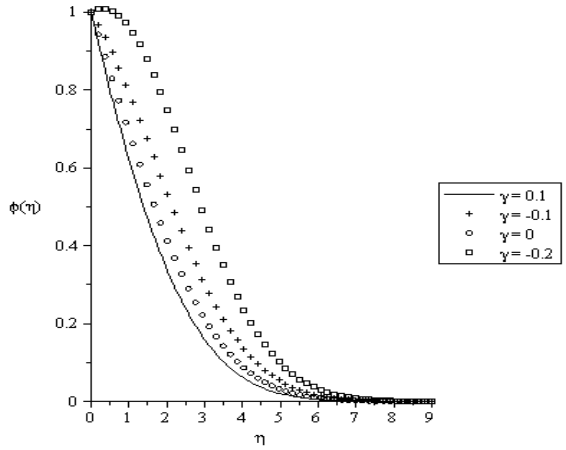

Figure 20: Concentration profiles for Ra = 0.1, G_T = 0.1, G_C = 0.1, S = 0, Pr = 0.71, Sc = 0.22, M = 0.1, D_f = 2, K = 0.1, Sr = 0.1, n = 1.

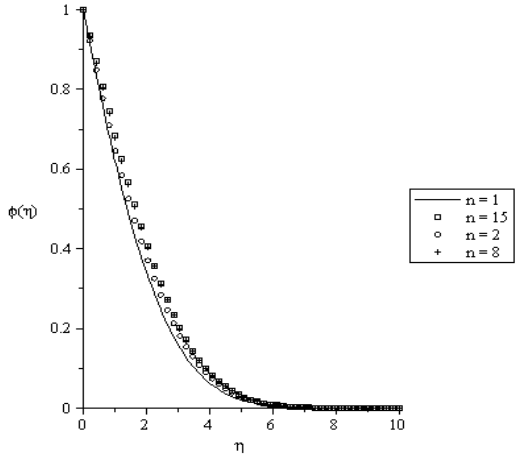

Figure 21: Concentration profiles for Ra = 0.1, G_T = 0.1, G_C = 0.1, S = 0, Pr = 0.71, Sc = 0.22, M = 0.1, D_f = 2, K = 0.1, Sr = 0.1, γ = 1.

Conclusions

In this paper we have studied numerically the effects of Soret, Dufour, chemical reaction, thermal radiation and volumentric heat generation/absorption on mixed convection stagnation point flow on an Iso-thermal vertical plate in porous media. The presented analysis has also shown that both temperature and concentration profiles are appreciably influenced by the Dufour and Soret effects. Therefore, we can conclude that for fluids with medium molecular weight (H_2, air), Dufour and Soret effects should not be neglected. Radiation, chemical reaction, and magnetic strength parameters have greater influence on the fluid velocity, temperature and concentration boundary layer thickness. It is interesting to note that the skin-friction and the rate of mass transfer increases, while the rate of heat transfer decreases with the increase in the rate of heat generation/absorption parameter *S*. Similarly, the fluid temperature and velocity increases with increase in the rate of heat generation/absorption parameter *S*. Finally, the order of the reaction has little influence on the concentration boundary layer thickness.

Acknowledgements

OPO would like to thank Covenant University, Ota, Nigeria for financial support for the research work.

References

[1] A. Bejan, I. Dincer, S. Lorente, A.F. Miguel, A.H. Reis, Porous and complex flow structures in modern technologies, Springer, New York. 2004.

[2] D.B. Ingham, I. Pop (Eds.), Transport phenomena in porous media, vol. II 2002, Pergamon, Oxford 1998.

[3] D.B. Ingham, I. Pop (Eds.), Transport phenomena in porous media, vol. III 2002, Elsevier, Oxford, 2005.

[4] K. Vafai, Handbook of porous media, Marcel Dekker, New York, 2000.

[5] K. Vafai, Handbook of porous media, second ed., Taylor and Francis, New York, 2005.

[6] G. Singh, P.R. Sharma, A.J. Chamkha, Effect of volumentric heat generation/absorption on mixed convection stagnation point flow on an Iso-thermal vertical plate in porous media, Int. J. Industrial Mathematics Vol. 2, No. 2 (2010) 59-71.

[7] A. Postelnicu, E. Magyari, I. Pop, Effect of a uniform horizontal through flow on the Darcy free convection over a permeable vertical plate with volumentric heat generation, Transport in porous media 80 (2009) 101-115.

[8] K. Vajravelu, A. Hadjinicolaou, Heat transfer in viscous fluid over a stretching sheet with viscous dissipation and internal heat generation, International Communication in Heat and Mass Transfer 20 (1993) 417-430.

[9] K. Vajravelu, J. Nayfeh, Hydromagnetic convection at a cone and a wedge, International Communication in Heat and Mass Transfer 19 (1992) 701-710.

[10] S. Shateyi, S.S. Motsa, P. Sibanda, The effects of thermal radiation, hall currents, Soret, and Dufour on MHD flow by mixed convection over a vertical surface in porous media, Mathematical Problems in Engineering, vol. 2010, Article ID 627475, 20 pages. Doi:10.1155/2010/627475.

[11] R.S.R. Gorla, I. Pop, Conjugate heat transfer with radiation from a vertical circular pin in non- Newtonian ambient medium, Warme Stoffubertr. 28 (1993) 11-15.

[12] A.A. Mohammadein, M.F. El-Amin, Thermal dispersion radiation effects on non-Darcy natural convection in a fluid saturated porous medium, Transport porous media 40 (2000) 153-163.

[13] H.M. Duwairi, R.M. Duwairi, Thermal radiation effects on MHD-Rayleigh flow with constant surface heat flux, Heat Mass Transfer 41 (2004) 51-57.

[14] S.R. Pop, T. Grosan, I. Pop, Radiation effects on the flow near the stagnation point of a stretching Sheet, Tech. Mech. 25 (2004) 100-106.

[15] T. Hayat, M. Mustafa, I. Pop, Heat and mass transfer for Soret and Dufour's effect on mixed convection

boundary layer flow over a stretching vertical surface in a porous medium filled with a viscoelastic fluid, Commun Nonlinear Sci Numer Simulat 15 (2010) 1183-1196.
[16] Z. Abbas, Y. Wang, T. Hayat, M. Oberlack, Mixed convection in the stagnation-point flow of a Maxwell fluid towards a vertical stretching surface, Nonlinear Analysis: Real World Applications, xx (In Press) xxx-xxx.
[17] M. S. Alam, M.M. Rahman, Dufour and Soret effects on mixed convection flow past a vertical porous flat plate with variable suction. Nonlinear Anal. Model. Control, 11, 3-12, (2006).
[18] A. Heck, Introduction to Maple, 3rd Edition, Springer-Verlag, (2003).

ABOUT THE AUTHORS

Olanrewaju, Philip Oladapo is a Senior Lecturer at the Covenant University, Ota, Nigeria. He is a member of Nigerian Association of Mathematical physics and Member of Nigerian Mathematical Society. He holds a Doctorate degree (PhD.) in Applied Mathematics from Ladoke Akintola University of Technology, Ogbomoso, Nigeria. His research interests are in Computational fluid dynamics.
Gbadeyan, Jacob A. is a Professor of Applied Mathematics at Covenant University (on sabbatical) and is the current Head of Department of Mathematics. He has his PhD in the University of Waterloo, Canada in Civil Engineering. He has supervised several PhD students in Applied Mathematics and Computer Science. He is into Applied Mechanics and Computational fluid Dynamics.

Nomenclature

g: Acceleration due to gravity of the Earth

G_T: buoyancy parameter $\left\{= \dfrac{Gr}{\mathrm{Re}^2}\right\}$

x, y: Cartesian coordinates

C_w: concentration at the plate surface

σ^* : Stefan-Boltzmann constant

K' : mean absorption coefficient

B_0: magnetic field of constant strength

D_f: Dufour number $\left\{= \dfrac{D_e k_T (C_w - C_\infty)}{c_s c_p (T_w - T_\infty)}\right\}$

Sr: Soret number $\left\{= \dfrac{D_e k_T (T_w - T_\infty}{T_m \alpha (C_w - C_\infty)}\right\}$

C_∞ : concentration in fluid far away from plate

C: concentration in the fluid

D_e: diffusion coefficient

F: dimensionless stream function

Gr: Grashof number $\left\{= \dfrac{g\beta(T_w - T_\infty)x^3}{\upsilon^2}\right\}$

Gr_M: modified Grashof number $\left\{= \dfrac{g\beta C_w x^3}{\upsilon^2}\right\}$

Nu: Nusselt number

$\widetilde{K}$: permeability of porous media

K: permeability parameter $\left\{= \dfrac{\upsilon}{\widetilde{K}c}\right\}$

Pr: Prandtl number $\left\{= \dfrac{\mu c_p}{k}\right\}$

S: rate of heat generation/absorption parameter $\{= -1, 0, 1, 2\}$

Re: Reynolds number $\left\{= \dfrac{U_\infty x}{\upsilon}\right\}$

Sc: Schmidt number $\left\{= \dfrac{\upsilon}{D_e}\right\}$

Sh: Sherwood number

c_p: specific heat at constant pressure

T: temperature of the fluid

T_∞ : temperature of fluid far away from plate

T_w : temperature of the plate

u, v: velocity components along x-and y-directions, respectively

Q: volumentric rate heat generation/absorption

k_1: rate of chemical reaction

c_s: concentration susceptibility

k_T: thermal diffusion ratio

n: order of reaction

σ_e : electrical conductivity of the fluid

Ra : radiation parameter $\left\{= \dfrac{4\sigma^* T_\infty^3}{\alpha K'}\right\}$

Greek Letters

β^* : coefficient of expansion with concentration

β : coefficient of thermal expansion

μ : coefficient of viscosity

k: coefficient thermal conductivity

ρ: density of fluid
ϕ : dimensionless concentration
η: dimensionless variable
υ: kinematic viscosity
ψ: stream function
γ: chemical reaction parameter

ϑ: dimensionless temperature

SUGGESTED CITATION

Olanrewaju, P.O.& Gbadeyan, J.A. 2011. "Effects of Soret, Dufour, chemical reaction, thermal radiation and volumentric heat generation/absorption on mixed convection stagnation point flow on an Iso-thermal vertical plate in porous media". *Pacific Journal of Science and Technology*. 11(2):XX-XX.